Hydrology Research

Hydrology Research Vol 55 No 12, 1197 doi: 10.2166/nh.2024.069

Evaluation of the effects of climatic variabilities on future hydrological scenarios: application to a coastal basin in Central Chile

Alejandra Camila Cortés Gonzalez [a,b], Hernán Alcayaga [a], Rossana Escanilla-Minchel [c,*], Mauricio Aguayo[d], Miguel Aguayo[e] and Camila Orellana[a]

[a] Faculty of Engineering and Sciences, Universidad Diego Portales, Santiago, Chile
[b] Department of Water Resources Management, Ministry of Public Works of Chile, Santiago, Chile
[c] School of Geography, University of Leeds, Leeds, UK
[d] Faculty of Environmental Sciences, Universidad de Concepción, Santiago, Chile
[e] Faculty of Natural Resources, Universidad Católica de Temuco, Santiago, Chile
*Corresponding author. E-mail: eeraem@leeds.ac.uk

ACC, 0009-0003-4011-8089; HA, 0000-0001-9300-0816; RE, 0000-0002-6441-5331

ABSTRACT

Evaluating the impacts of climate change on coastal basins with a Mediterranean climate represents a significant challenge concerning water security. Consequently, an assessment was conducted on the effects of climate change on hydrological components in a basin within the Coastal Mountain Range of Central Chile. The hydrological model SWAT+ was used, forced by two Shared Socioeconomic Pathways (SSP2-4.5 and SSP5-8.5), incorporating a downscaling process and analyzing both extreme and non-extreme events. Climate projections were made for the following three periods: near (2015–2030), middle (2015–2060), and distant (2015–2100) future. Results indicate a consistent rise in average temperatures across all periods, coupled with decreased precipitation for most of the year. Particularly in the distant future, austral summer stands out as the most impacted season, with projections showing a substantial decrease in precipitation (27 and 54% for SSP2-4.5 and SSP5-8.5, respectively), accompanied by significant increases in both maximum and minimum temperatures. Moreover, the streamflow is anticipated to decline considerably in the austral autumn (−8 and −83% for SSP2-4.5 and SSP5-8.5, respectively). Additionally, as consequences of climate change an increase in droughts (during the dry season) and flooding problems (during the wet season) are expected in the basin, increasing the risk for both extremes.

Key words: coastal basin climate change, components of hydrological cycle, hydrological modeling

HIGHLIGHTS

- Procedure for evaluating climate projections in a basin.
- Impacts of climate change in coastal basins with a Mediterranean climate.
- Short-, medium-, and long-term climate projections of precipitation, flow, maximum and minimum temperature are presented.
- Long-term hydrological components are evaluated on a seasonal and monthly basis.

1. INTRODUCTION

Water is one of the natural resources most affected by the effects of climate change, having direct implications on people's lives, the ecosystem, and the global economy (Escanilla-Minchel *et al.* 2020; Muñoz *et al.* 2020a). One of the most evident manifestations of climate change is its influence on the water balance and hydrological processes throughout the world (Ha *et al.* 2019). The latter suggests that water resource management must focus on a preventive approach for adaptation to climate change, incorporating the knowledge of the close relationships between the hydrological cycle and climate (Ha *et al.* 2019).

Climate change is attributable to human activities that have altered the composition of the global atmosphere, this added to the natural variability of the climate observed during comparable periods (Calvin *et al.* 2023). According to the IPCC, human influence on climate has been the dominant cause (with a 95% probability or greater) of more than half of the observed increase in global mean surface temperature in the period 1951–2010. The latter has caused sea-level rise (Koutsoyiannis

2020), ocean warming, rapid ice and snow melting, and changed the frequency or intensity of climatic extremes in the second half of the 20th century (IPCC 2014). Assessment of the effects of these climate variations, at a local and regional scale, reflects the need to improve the abilities to estimate the hydrological process variability at the basin scale (Lu *et al.* 2010). Using hydrological models plays an essential role in identifying the current and future effects of climate change, generating scenarios that allow us to adopt mitigation measures (Pérez-Sánchez *et al.* 2020).

Since 2010, Chile has experienced one of the most severe droughts of the last century. The so-called mega-drought (Garreaud *et al.* 2020), combined with intensive agricultural and forestry activities and the current water management system, has caused water scarcity, particularly in the Mediterranean and semi-arid regions of Chile (Muñoz *et al.* 2020a). The conflicts over water in Chile have deepened in the last 10 years, involving the legal, political, economic, social, and environmental spheres (Bauer 2015).

Assessing the impacts of climate change on Mediterranean river basins is a huge challenge, as these basins are characterized by a marked annual cycle, with dry summers and very wet winters (Essa *et al.* 2023), which can lead to such basins experiencing a wide range of natural and anthropogenic threats to water security. Threats include severe droughts and extreme floods, seawater intrusion into coastal aquifers, degradation of fertile soils, and desertification due to poor and unsustainable management (Vozinaki *et al.* 2018). It should be noted that Mediterranean droughts, particularly those that occur during the wet season, can have a strong impact on water resources by reducing groundwater (GWQ) levels and the water available in dams and reservoirs (Tramblay *et al.* 2020).

On a local scale, some studies show how climate change can be added as an additional stress factor within the center-south of Chile (Barrientos *et al.* 2020) and these new conditions are more critical for the Cordillera de la Costa basins in central Chile (Stehr *et al.* 2008; Torres *et al.* 2015). Valdés-Pineda *et al.* 2014 using the PRECIS model have predicted a reduction between 60 and 70%, compared to the current regime for the Maule (34°41′–36°33′ S) and the Los Lagos (40° 13′–44° 3′ S) regions, being more intense during the austral spring season (i.e. October to December).

Despite significant efforts in this regard, some questions remain unanswered, particularly for the Mediterranean river basins in Chile. One of the most critical gaps is related to how much rainfall and temperatures will increase or decrease in the basin, and how the hydrological cycle will be affected by climate change. Also, how much will the flow of the streams decrease if the trend of reduced rainfall – such as the current one – continues to increase? On the other hand, other doubts arise, such as: What will be the months of greatest floods to make decisions in terms of water management? In which seasons of the year will the greatest drought be experienced? Will the effects of climate change be seen in the short, medium or long term? In the event that no changes are made to mitigate climate change, how will rainfall, discharge, max and min temperature be affected? The answers to these questions would be of great support to water resource managers and private and public entities to develop preventive approaches to climate change adaptation in coastal basins located in the south-central region of Chile.

The objective of this work is to evaluate the effects of climate change on hydrologic processes in a Mediterranean-climate river basin in the Cordillera de la Costa of south-central region of Chile, for near (2015–2030), medium (2015–2060), and far future (2015–2100), considering the Shared Socioeconomic Pathway (SSP2-4.5 and SSP5-8.5) scenarios. To achieve this, the SSP2-4.5 and SSP5-8.5 are spatially downscaled using the Quantile Mapping Bias Correction method (Escanilla-Minchel *et al.* 2020) and subsequently analyzed to verify the accuracy by comparing historical observed data and GCM outputs in the period 1979–2015. Such bias-corrected scenarios provide precipitation and temperature projections at a regional scale as input data to a hydrological model that quantifies the changes in hydrological dynamics of the basin. The hydrological model used was SWAT+ (Bieger *et al.* 2017) and the output results are associated with climate change on hydrologic components discharge, evapotranspiration (ET), percolation (PERC), surface runoff (SURQ), GWQ, and water yield (WYLD).

2. METHODS

2.1. Study area

The study area is located in the coastal zone of south-central Chile and corresponds to the Andalién River basin (Figure 1). This basin drains from the western slope of the Cordillera de la Costa, between 36°42′ and 36°56′ S and between 72°36′ and 73°04′ W. The basin area delimited at the *Río Andalién Camino a Penco* streamflow gauging and meteorological stations (7 m.a.s.l.), close to the outlet, is 751.2 km². The Andalién River is 36 km long and outlet flows are discharged into the

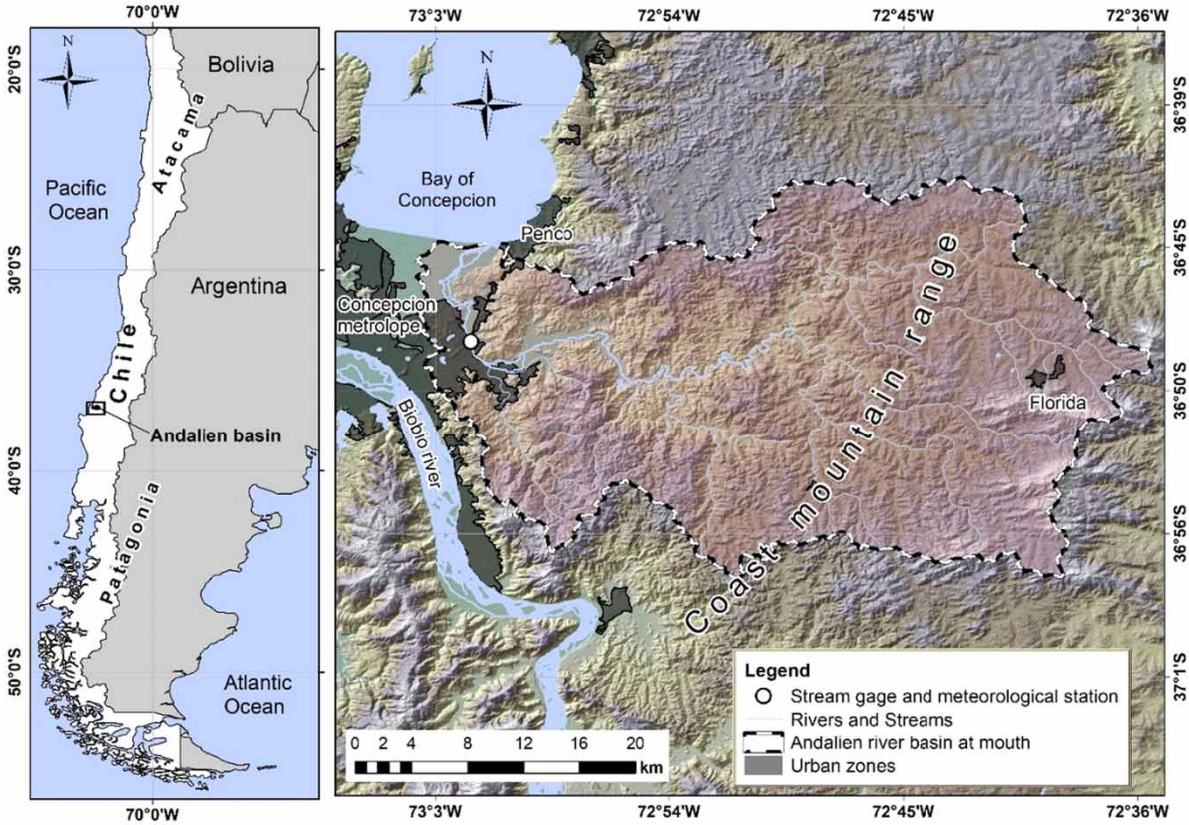

Figure 1 | Location of the Andalién River basin in the geographic context.

Bay of Concepción, before crossing the metropolitan area of the city of Concepción, and total inhabitants in the basin is 272,254. The basin maximal altitude is 567 m.a.s.l. (Castillo 2008).

According to the Chilean General Directorate of Waters (DGA), the Andalién River basin is under the influence of a Mediterranean bioclimate (DGA 2004), while according to the Koppen-Geiger classification, the climate in the basin is warm temperate, with four well-marked cold and humid months (Kottek *et al.* 2006). More than 70% of the annual precipitation in the basin occurs between May-August (winter months), when the annual mean precipitation ranges between 1,200 and 1,400 mm. The average temperature is 13 °C, with thermal amplitudes of 8.1 °C (Castillo 2017).

The main soil types in the basin are granitic rocks, characterized by their low permeability and abundant porosity (Stolpe 2006) which favors the surface runoff generation through the mechanism of infiltration excess (Horton 1933; Morbidelli *et al.* 2018). According to the National Forestry Corporation (CONAF), the dominant land use/land cover (LULC) corresponds to non-native adult and young plantations (60.7%), followed by native forest and mixed forest (17.0%), agriculture (8.3%), grasslands (7.0%), urban and industrial areas (3.9%), areas without vegetation (2.7%) and other uses (0.5%) (CONAF 2015; Orellana *et al.* 2022).

2.2. Hydrological model

The hydrological model used in this study is the Soil and Water Assessment Tool Plus (SWAT+) (Arnold *et al.* 1998) developed by the United States Department of Agriculture (USDA). SWAT+ is a physically-based model that works in a continuous-time interval (Wu *et al.* 2020) and allows simulating hydrologic processes and water quality. The model works on a semi-distributed processes basis designed to calculate water routing, sediment loads, and concentration of nutrients (Eckhardt *et al.* 2005). Also, the model has been used in several studies involving the effects of climate change on water resources (Wangpimool *et al.* 2013).

SWAT+ requires two types of spatially distributed input data and hydro-climatic time series. Spatial data includes a digital elevation model (DEM), LULC and soil type. LULC was obtained through the analysis of satellite images from Landsat 5 and

8 sensors (base on (Orellana *et al.* (2022)) and the LULC classes of the basin were assigned in equivalence to those of the SWAT+ model: FRST (Native and Mixed Forest), FRSE (Adult Plantation), RNGB (Young Plantation), AGRL (Agricultural Coverage), UIDU (Industrial and Urban Zone), RNGE (Thickets and Prairie), BARR (Soil devoid of vegetation), WETN (Wetlands), and WATR (Surface Water Bodies).

The time series includes hydro-climatic data as precipitation, solar radiation, relative humidity, wind speed, and temperature (Welde & Gebremariam 2017). SWAT+ also has a weather generator tool that allows gap-filling missing data during certain periods of time in the simulation cycle. The latter is achieved by providing long-term daily data of precipitation and maximum and minimum temperatures (Mengistu *et al.* 2019).

SWAT+ is more adaptable than SWAT in terms of spatial representation (Wu *et al.* 2020) and code flexibility. This semi-distributed model works by dividing a watershed into several sub-watersheds, which are then subdivided into hydrological response units (HRUs). Such HRUs are composed of soil types, slopes range grouped, and similar LULC (Ayivi & Jha 2018).

2.2.1. Calibration and validation of the hydrological model SWAT +

Calibration is performed by modifying some model parameters and comparing the simulated streamflow with the observed data. Eleven parameters are used for this process, based on Orellana *et al.* (2022). Such parameters have been widely used in several studies in different countries (Verichev *et al.* 2020) and also in Chile (Tan *et al.* 2017).

The most relevant parameter from the sensitive model output is CN2 (Curve Number for humidity II conditions). This parameter directly affects the amount of runoff generated, which finally has an important influence on the streamflow. The second most sensitive parameter of the model is ALPHA_BF (Alpha Factor of the base flow), which directly controls the base flow and the amount of water that is discharged into the aquifer. The third parameter is SOL_AWC1 (Water Holding Capacity), which controls the amount of evaporation from the soil, the fourth parameter is SOL_K1 (Hydraulic Conductivity), which influences the amount of water that infiltrates into the soil and the last parameter is GWQMN (Minimum Depth for Return Flow) which is related to the amount of GWQ that discharges into rivers.

The calibration and validation periods comprise evaluating the model performance in 5 years (2003–2007) and nine years (2008–2016), respectively.

The optimal values for the calibration parameters and the average of each parameter for each year are detailed in Table 1. In the validation period, five sets of parameters obtained in each model were evaluated, as well as their average.

To evaluate the model performance for both periods (calibration and validation), four statistical indicators are used. These indicators are coefficient of determination (R^2), the Nash–Sutcliffe efficiency (NSE), the percentage bias (PBIAS) and the Kling–Gupta efficiency (KGE) (Brouziyne *et al.* 2017). The change criteria associated with these four indicators are the same as those classified by Kouchi (Kouchi *et al.* 2017).

2.3. Generation of climate change scenarios

SSP2-4.5 and SSP5-8.5, GCM selection and downscaling process.

GCMs are mathematical models that seek to represent the climate system of the Earth (Lee *et al.* 2014). The models simulate the planetary atmosphere and ocean circulation processes and have been used in several studies (Oti *et al.* 2020). To estimate the climate change effects on the water balance in the Andalién River basin, simulated climate change data from GCM are obtained. After that, a statistical downscaling process is performed to the GCM data to be incorporated into the hydrological model. The downscaling process allows the spatial resolution scale of the GCMs to be improved from a global to a regional scale and to generate hydrological projections through a selected hydrological model (Bae *et al.* 2011), for this case applying the SWAT+ model.

The Intergovernmental Panel on Climate Change (IPCC) has determined four greenhouse gas emission scenarios in the Sixth Assessment Report (AR6): Climate Change of 2022, known as the SSP5-8.5, SSP3-7.0, SSP2-4.5, and SSP1-2.6 (IPCC 2023).

For this study, two scenarios are considered: medium (SSP2-4.5) and high (SSP5-8.5) (Luo *et al.* 2019). The SSP2-4.5 scenario represents the development of the middle of the road where socioeconomic factors follow their historical trends without significant changes, while SSP5-8.5 represents the worst-case scenario with the upper end of the range of future roads. These two scenarios were selected as they offer contrasting pathways that are relevant to studying potential impacts and policy implications across a range of sectors. (Kassaye *et al.* 2024).

Table 1 | Calibration parameters for the SWAT model

Parameter	Description	Range	2003	2004	2005	2006	2007	Average	
MGT1	CN2	Initial SCS runoff curve number for moisture condition II		−85%	−80%	−62%	−62%	−80%	−74%
GW	GW_DELAY	Groundwater delay time (days)	[0–400]	45	10	40	40	10	29.00
	ALPHA_BF	Baseflow alpha factor (days)	[0,1–0.3] [0.9–1]	0.1	0.95	0.2	0.2	0.9	0.47
	GWQMN	Threshold depth of water in the shallow aquifer required for return flow to occur (mm H_2O)	[0–5,000]	250	0.1	7	7	1	53.02
	GW_REVAP	Groundwater 'revap'coefficient	[0.02–0.2]	0.02	0.02	0.05	0.05	0.05	0.04
	REVAPMN	Threshold depth of water in the shallow aquifer required for 'revap' or percolation to the depth aquifer to occur (mm H_2O)	[0–500]	250	100	11	11	0.3	74.46
	RCHRG_DP	Deep aquifer percolation fraction	[0–1]	1	0.47	0.5	0.5	0.2	0.53
HRU	HRU_SLP	Average slope steepness (m/m)		−10%	−50%	92%	92%	2%	25%
	OV_N	Manning's '*n*' value for overland flow	[0.01–0.41]	0.3	0.25	0.41	0.41	0.25	0.32
	CANMX	Maximum canopy storage (mm H_2O)	[0–100]	10	0	15	15	0	8.00
	ESCO	Soil evaporation compensation factor	[0.01–1]	0.4	0.2	0.2	0.2	0.01	0.20
	EPCO	Plant uptake compensation factor	[0.01–1]	0.7	0.1	0.8	0.8	1	0.68
SOL	SOL_Z1	Depth from soil surface to bottom of layer (mm)		−71%	−81%	−70%	−70%	−81%	−75%
	SOL_BD1	Moist bulk density (Mg/m3 or g/cm3)	[1.1–1.9]	1.39	1.9	1.29	1.29	1.9	1.55
	SOL_AWC1	Available water capacity of the soil layer (mm H_2O/mm soil)	[0–1]	0.4	0.16	0.4	0.4	0.16	0.30
	SOL_K1	Saturates hydraulic conductivity (mm/h)	[0 – 2,000]	33	1.75	33	33	1.75	20.50
RTE	CH_N2	Manning's '*n*' value for the main channel	[−0.01–0.3]	0.15	0.3	0.15	0.15	0.3	0.21
	CH_K	Effective hydraulic conductivity in the main channel alluvium (mm/h)	[−0.01–500]	1.81	1	1.81	1.81	1	1.49

Based on the greenhouse gas emission scenarios, there is a set of several GCMs developed by different working groups worldwide. The combination of analysis of these models could provide a better evaluation of the water resources than a single GCM (Pierce *et al.* 2009). Therefore, it is preferable to use the ensemble modeling approach rather than a single model simulation (Ehsan *et al.* 2019).

A model ensemble has been shown to provide high confidence and optimally quantify uncertainties in future climate projections (Tebaldi & Knutti 2007). In this study, the precipitation data, daily maximum and minimum temperatures of an ensemble of eight models from the Coupled Model Intercomparison Project Phase 6 (CMIP6) are analyzed (Table 2). These were selected according to the availability of GCMs in Infrastructure for the European Network for Earth System Modelling database (Is-Enes 2021) and their adjustment to the observed data average.

Table 2 | Summary of global circulation model ensemble used

GCM	Institution/Center	Nominal Resolution	Ensemble Member
ACCESS-CM2	Australian Community Climate and Earth System Simulator (ACCESS)	250 km	r1i1p1f1
ACCESS-ESM1-5	Australian Community Climate and Earth System Simulator (ACCESS)	250 km	r13i1p1f1, r15i1p1f1
INM-CM4-8	Institute of Numerical Mathematics (INM)	100 km	r1i1p1f1
MRI-ESM2-0	The Meteorological Research Institute (MRI)	100 km	r5i1p1f1
IPSL-CM6A-LR	Institut Pierre Simon Laplace – Climate Model Version 6 (IPSL-CM6-LR)	250 km	r14i1p1f1
CanESM5	Canadian Centre for Climate Modelling and Analysis Earth System Model version 5 (CanESM5)	500 km	r10i1p1f1, r19i1p2f1

A GCM model includes ten to twenty atmospheric layers and sometimes up to thirty layers on the oceans (IPCC 2014). By default, the horizontal resolution in these models ranges between 250 and 600 km. Therefore, a downscaling process is required to represent from a coarse-scale atmospheric information to a regional or local scale (von Storch *et al.* 1993). Also, the purpose of this is to identify possible biases between observed and simulated climate variables, which constitute the basis for correcting future GCM projections (Chen *et al.* 2019), reaching up to a basin-scale projection. Bias correction uses transformation algorithms, depending on the downscaling method used to adjust the result of the GCM.

In this study, a statistical downscaling through the Quantile Mapping Bias Correction method is performed (Escanilla-Minchel *et al.* 2020). This method is comparatively efficient from a computational point of view, easily transferable to other regions, and it is based on standard and accepted statistical procedures (Fowler *et al.* 2007).

In the downscaling process, two meteorological time-series datasets in two subsequent periods have been used: (i) observed and simulated historical period and (ii) projected period, which includes daily precipitation and maximum and minimum temperature data. The first period includes both observed data from 1979 to 2014 obtained from the Río Andalién Camino a Penco meteorological station and GCM simulations output data. The second period includes an ensemble of GCM projected climate data from 2015 to 2100 obtained from Is-Enes (2021).

The downscaled ensemble of meteorological data projections for each SSP is entered into the SWAT+ hydrological model, already calibrated and validated. In this way, the potential climate change effects on the hydrologic processes in Andalién river basin are obtained.

The overall modeling framework for the evaluation of climate change effects on hydrologic components in a Mediterranean-climate river basin is shown in Figure 2.

3. RESULTS

3.1. Calibration and validation of the SWAT+ model

Applying the SWAT+ model in the Andalién river basin, a total of 27 sub-basins was delineated considering a threshold of 1,500 ha, based on a comparison with regional hydrographic maps. The number of HRUs varied between 268 and 326 HRUs, according to the combinations between soil type, terrain slope classification (0–15%, 15–30%, and 30–100%), and LULC.

The entire simulation period was divided into an 8-year spin-up period (1994–2002), followed by a 5-year calibration period (2003–2007) and a 9-year validation period (2008–2016). For each calibration year, a model with its respective land use map and a set of calibration parameters was generated with the corresponding year.

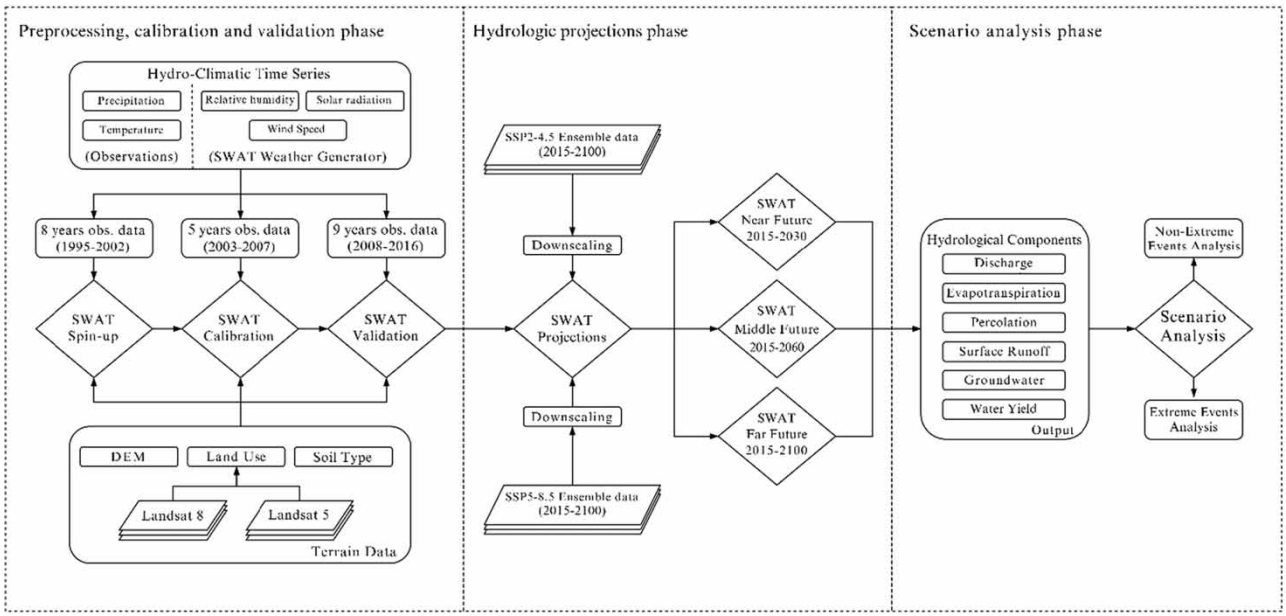

Figure 2 | Modeling framework for the evaluation of climate change effects on hydrologic components in a Mediterranean-climate river basin.

In the validation period, five sets of parameters obtained in each model were evaluated, as well as their average (Figures 3(b) and 3(c)).

Figure 3(a) shows the hydrograph during the calibration and validation period at the Río Andalién Camino a Penco station. We can see that, for the calibration period, from 2003 to 2004, the maximum discharges are overestimated, and subsequently, from 2005 to 2007, the results have a better fit. In the validation period, we can see that from 2008 to 2013, in wet periods there is a discharge overestimation and in dry periods there is an underestimation. From 2013 to 2015 there is a general underestimation of simulated discharge. In Figures 3(b) and 3(c), we can see how the obtained discharge in the calibration (Figure 3(b)) has a better fit for low discharge and a greater dispersion for high discharge. This is much more accentuated in the validation period (Figure 3(c)).

4. PERFORMANCE ANALYSIS OF THE BIAS CORRECTION METHOD FOR THE OBSERVED HISTORICAL PERIOD 1979–2005

The historical observed mean daily time series of precipitation and temperatures are compared with the mean daily historical data of the GCM for the same period (1979–2014). The goal of this process is to verify if the bias correction method is performing correctly. Subsequently, the observed historical data are contrasted with daily averages of the GCM projections SSP2-4.5 and SSP5-8.5 also to evaluate the bias correction.

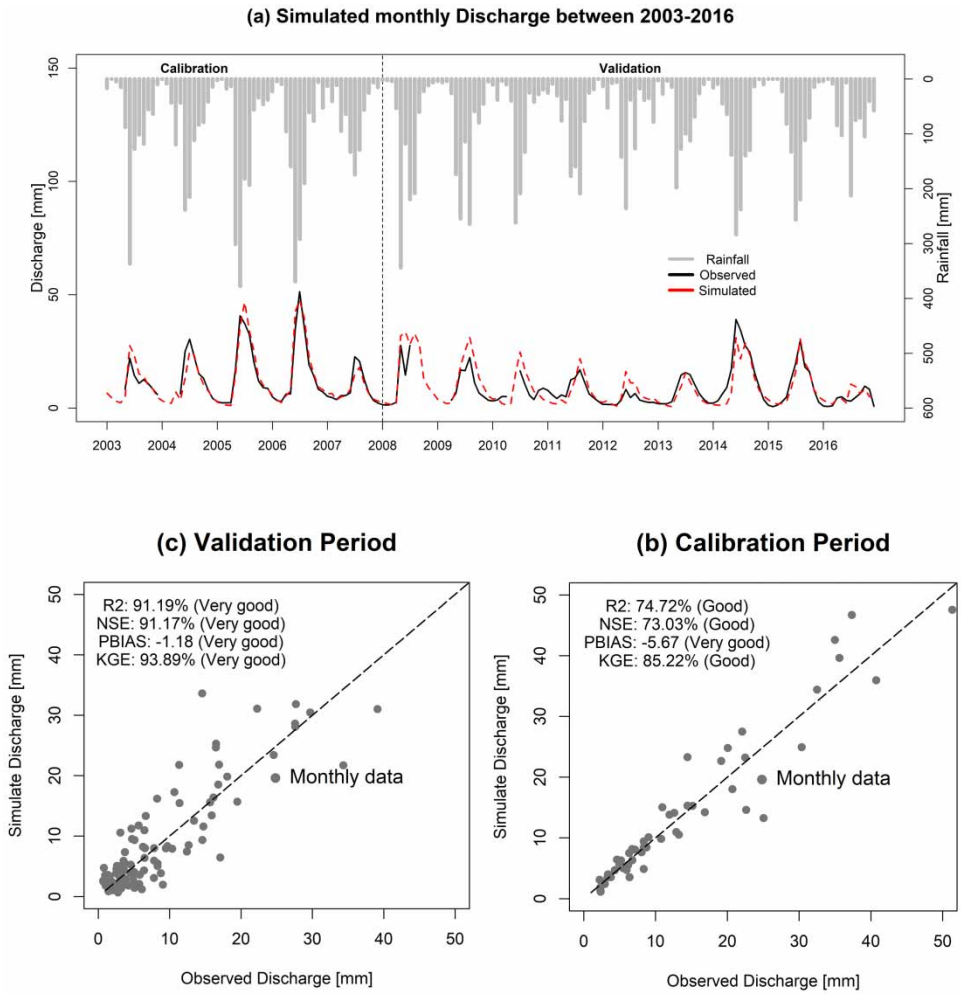

Figure 3 | (a) Observed and simulated monthly discharge for calibration and validation periods. (b) Scatter plot of observed and simulated monthly discharge for calibration periods. (c) Scatter plot of observed and simulated monthly discharge for validation periods.

4.1. Historical

For the precipitation time series, maximum and minimum daily mean temperatures, we can see that the adjustment of the historical period of the GCM with the observed data is efficient after applying the bias correction method, since the values of RMSE and MSE in precipitation are 0.18 and 0.03, respectively, and for minimum and maximum temperature the values of RMSE and MSE are less than 1.15×10^{-15}.

4.2. Projections

When comparing daily averages of projected precipitation and observed time series data (Figures 4(a) and 4(b)), we can see that the bias correction is not as efficient as with the simulated historical series (Figure 6), which typically occurs when

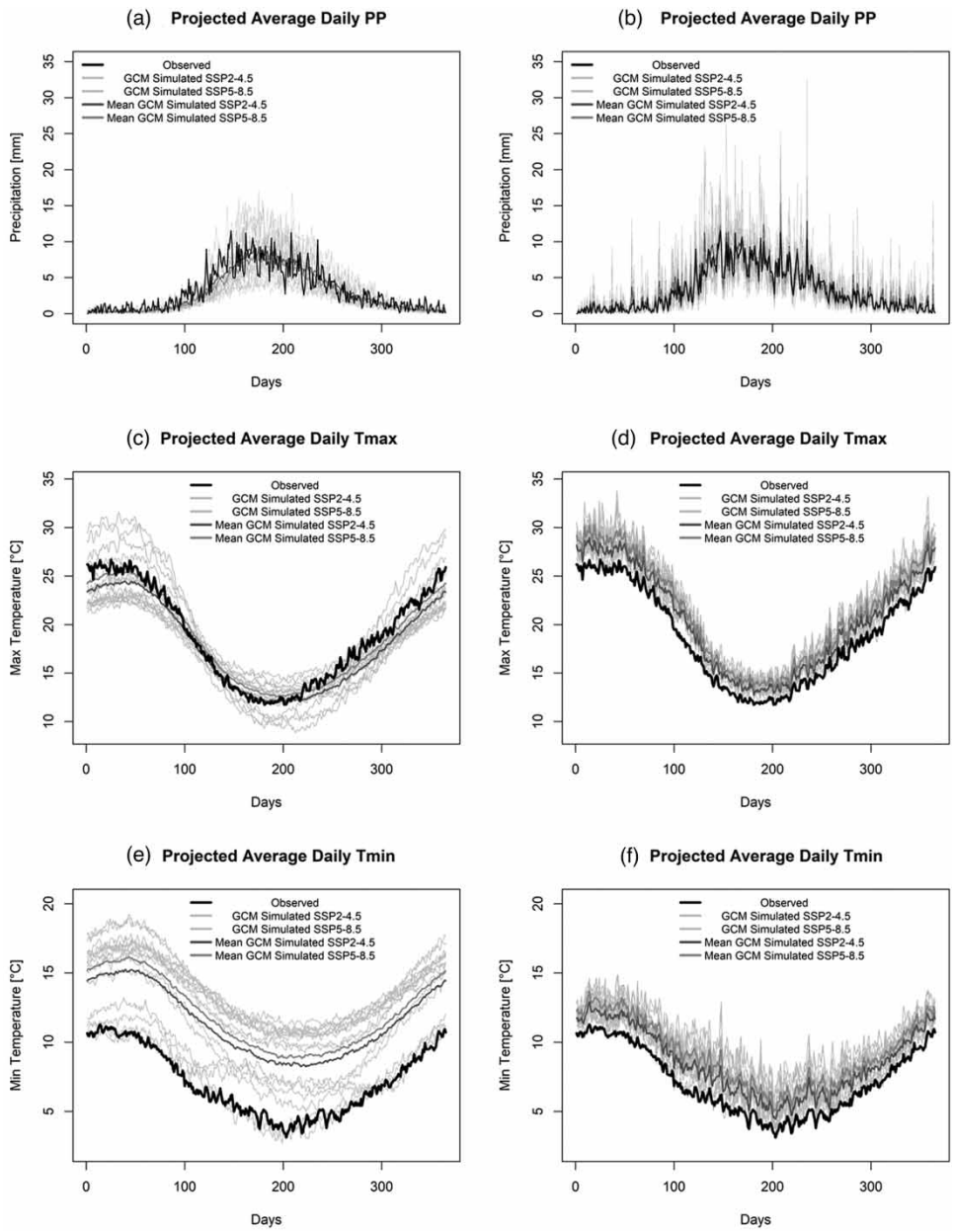

Figure 4 | (a) Observed and projected precipitation without bias correction. (b) Observed and projected precipitation with bias correction. (c) Averages of maximum temperatures projected without bias correction and (d) averages of maximum temperatures projected with bias correction. (e) Averages of projected minimum temperatures without bias correction. (f) Averages of historical minimum temperatures with bias correction.

projected data are compared with observed data (Escanilla-Minchel *et al.* 2020). It should be noted that at the daily scale, precipitation increases by 9.31% for SSP2-4.5 and decreases by 2.28% for SSP5-8.5.

The daily GCM averages of the maximum and minimum temperature projections (SSP2-4.5 and SSP5-8.5) are shown in Figures 4(c)–4(f). Here, we can see that after the correction of the bias, there is a generalized increase in the maximum and minimum temperatures, which in maximum temperature is 8.61 and 12.63%, for SSP2-4.5 and SSP58.5, respectively, and that in the case of the minimum temperature is 17.83 and 24.63%, for SSP2-4.5 and SSP58.5, respectively, which shows that the increase in average temperature that we observe is produced especially by the increase in minimum temperature. This is consistent with the study by Glynis *et al.* 2021, which concludes that the maximum temperature is not increasing as much as the minimum temperature (in daily scale) (Glynis *et al.* 2021).

4.3. Verification

The observed data and the data projected by SSP2-4.5 and SSP5-8.5 were compared for the period from 2016 to 2020, to check the effectiveness of the projections already made.

Figure 5(a), where the observed and projected precipitation data are compared, shows that the average projected precipitation is greater than the observed data, which is 31.87% for SSP2-4.5 and 34.22% for SSP5-8.5, which is mainly due to the increase in extreme events expected in the future (Ghosh & Mujumdar 2008; Gouveia *et al.* 2022).

Figure 5(b) shows that the projected maximum temperature follows practically the same trend as the observed data, with a percentage difference of 1.15% in SSP2-4.5 and 0.97% in SSP5-8.5. Whereas Figure 5(c) shows that within the minimum temperatures, the observed temperature is always higher than the simulated temperature and the lower temperatures are always lower than the simulated ones, which translates into a percentage difference of 8.69% in SSP2-4.5 and 9.62% in SSP5-8.5.

4.4. Table with primary statistics on the observed, verified (by the GCM) and predicted (by the GCM)

In Table 3, you can see that the asymmetry in the maximum temperature tends to be negative, which implies that the smallest extremes are far from the mean, while the precipitation and minimum temperature tend to be positive, which implies that the largest extreme values are further away from the mean.

On the other hand, in kurtosis, the verification periods tend to deliver negative values, which implies that there are fewer extreme values, while the simulation periods tend to deliver positive values which indicates that there are more extreme values.

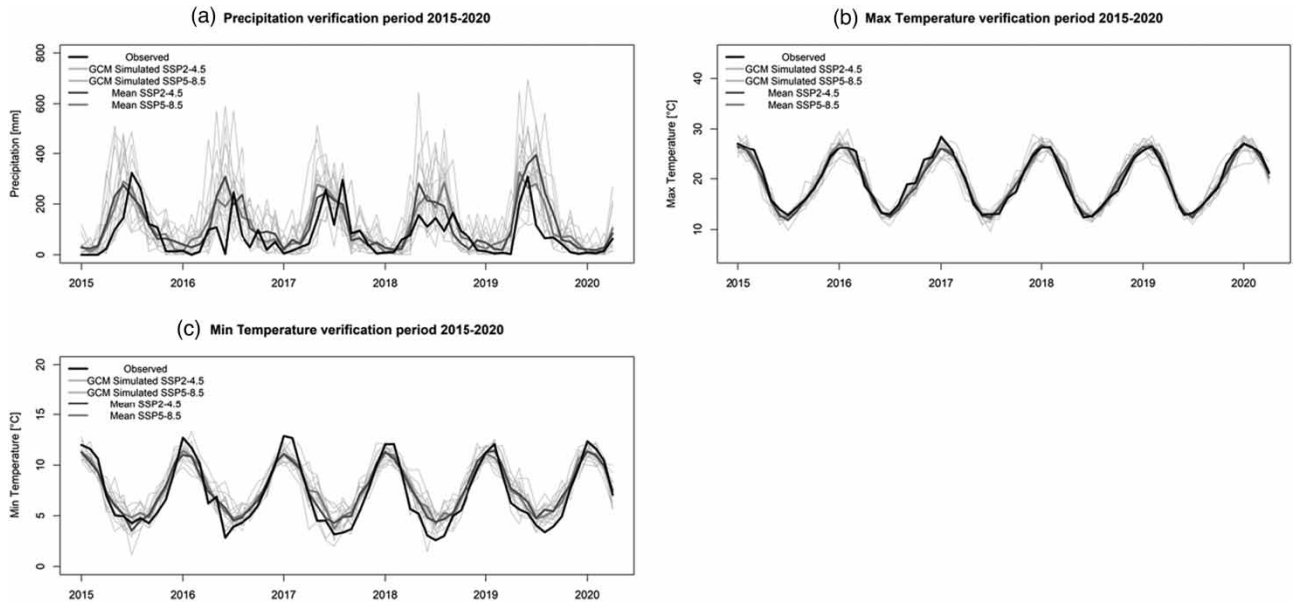

Figure 5 | (a) Precipitation verification period 2015–2020. (b) Max. temperature verification period 2015–2020. (c) Min. temperature verification period 2015–2020.

Table 3 | Primary statistics on the observed, verified (by the GCM) and predicted (by the GCM) data

		Observed Data		Data Projected SSP2-4.5		Data Projected SSP5-8.5	
		Historical Period (1979–2014)	Verification Period (2015–2020)	Verification Period (2015–2020)	Simulated Period (2015–2100)	Verification Period (2015–2020)	Simulated Period (2015–2100)
PP	Mean	1,121.99	824.47	1,443.99	1,278.62	1,413.62	1,278.62
	Standard deviation	265.80	386.49	175.16	143.49	75.26	143.49
	Skewness	0.05	−0.96	0.62	0.55	0.16	0.55
	Kurtosis	−0.99	−0.75	−1.28	0.18	−1.38	0.18
	Autocorrelation at lag-1	0.01	0.01	−0.41	0.23	−0.46	0.23
	Autocorrelation at lag-10	−0.19	*NA*	*NA*	0.14	*NA*	0.14
	Autocorrelation at lag-30	−0.06	*NA*	*NA*	−0.01	*NA*	−0.01
T_{max}	Mean	19.17	20.43	19.37	20.49	19.42	20.49
	Standard deviation	0.35	2.24	0.27	0.70	0.20	0.70
	Skewness	−0.58	1.29	−0.18	−0.30	0.15	−0.30
	Kurtosis	−0.02	−0.19	−2.05	−1.22	−1.93	−1.22
	Autocorrelation at lag-1	−0.14	−0.01	0.52	0.92	−0.08	0.92
	Autocorrelation at lag-10	0.23	*NA*	*NA*	0.67	*NA*	0.67
	Autocorrelation at lag-30	−0.02	*NA*	*NA*	0.03	*NA*	0.03
T_{min}	Mean	6.79	7.57	7.54	8.50	7.61	8.50
	Standard deviation	0.29	1.39	0.22	0.57	0.13	0.57
	Skewness	−0.42	1.30	0.08	−0.34	−0.42	−0.34
	Kurtosis	0.89	−0.19	−1.61	−1.11	−1.18	−1.11
	Autocorrelation at lag-1	−0.21	−0.05	0.20	0.92	−0.13	0.92
	Autocorrelation at lag-10	−0.11	*NA*	*NA*	0.63	*NA*	0.63
	Autocorrelation at lag-30	−0.09	*NA*	*NA*	0.03	*NA*	0.03

In the 30-year autocorrelation, a decrease in rainfall is shown, but on the other hand, for the maximum and minimum temperature, an increase in the values is observed.

5. CLIMATE CHANGE PROJECTIONS WITHOUT CONSIDERING EXTREME EVENTS

It is likely that the occurrence of extreme events, such as floods, heat waves and droughts, will intensify because of the climate change (Githui *et al.* 2009). Figure 6 shows that extreme precipitation values projections influence the results of the

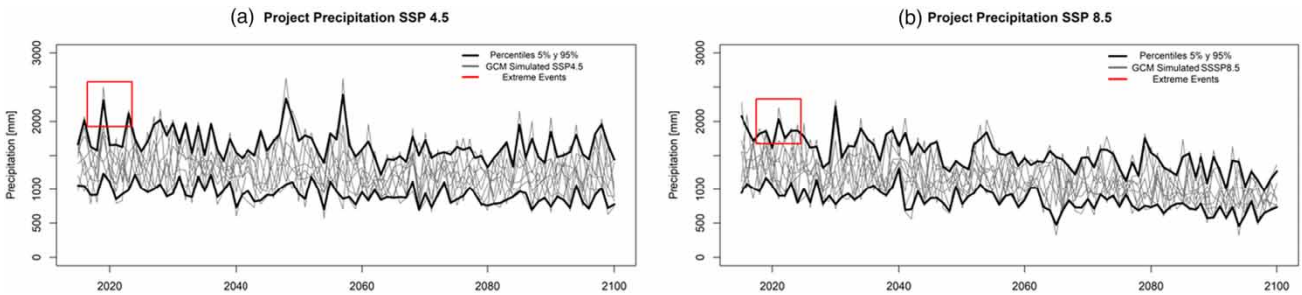

Figure 6 | (a) Projected precipitation of an ensemble of 10 GCMs in SSP2–4.5 and (b) projected precipitation of 10 GCMs in SSP5-8.5.

hydrologic components delivered by the models. To consider the uncertainty associated with extreme events, the 5 and 95% percentiles are used, eliminating the values that are outside this range, as seen in Figures 6(a) and 6(b).

Four average time periods are also defined that represent a specific year, the first period is from 2010 to 2015, which is represented in the year 2015, the second period is from 2027 to 2030, which is represented in the year 2030, the third period is from the year 2057 to 2060, which is represented in 2060 and finally the fourth period is from the year 2097 to 2100, which is represented in the year 2100.

The representative year 2015 is observed data and the other three representative years are GCM simulated data. Considering the difference between these representative years, we define three periods called near future (2015–2030), middle future (2015–2060) and far future (2015–2100).

5.1. Analysis of the results for the near (2025), medium (2050), and far future (2100)

The precipitation, discharge and maximum and minimum temperature projection results for SSP2-4.5 and SSP5-8.5 in the period 2015–2100 are shown in Figure 7. For both discharge and precipitation, a decrease is estimated as shown in Figures 7(a) and 7(b). For the temperature projections, the trends are upward for both maximum and minimum (Figures 7(c) and 7(d)). Also, we observed a variation in maximum temperature greater than the minimum temperature for the year 2100 in both SSP2-4.5 and SSP5-8.5.

Figure 7 shows that, for the three periods, the precipitation and temperature projections are more unfavorable in SSP5-8.5 than in SSP2-4.5. In SSP2-4.5, as time advances, there is a tendency to decrease precipitation between the near future and the middle future, rising again in the far future. Temperatures always maintain an increasing trend, while precipitation trend in SSP5-8.5 always decreases as the temperatures increases in the three periods.

Figure 7(a) shows a steady decrease in precipitation, which is much more accentuated in the average rainfall of the 8 GCMs of the SSP5.8.5 than in the average GCM of the SSP2-4.5, with the difference between them being 30%. This is reflected in Figure 7(b), which shows a similar trend to precipitation, because one of the most important factors in the flow is the precipitation of the basin.

On the other hand, in Figure 7(c), a pronounced increase in the maximum temperature is observed, but it is even greater in SSP5-8.5 than in SSP2-4.5, with the difference between them in the year 2100 being approximately 2.6 °C. On the other hand, for the minimum temperature, the temperature increase is not as pronounced and the difference between SSP5-8.5 and SSP2-4.5 is 2.0 °C.

From this it can be concluded that, on an annual scale, the increase in the average temperature is due to the pronounced increase in the maximum temperature, since by the year 2100, the maximum temperature increases by 5.2 °C, while the minimum temperature increased by 4.2 °C.

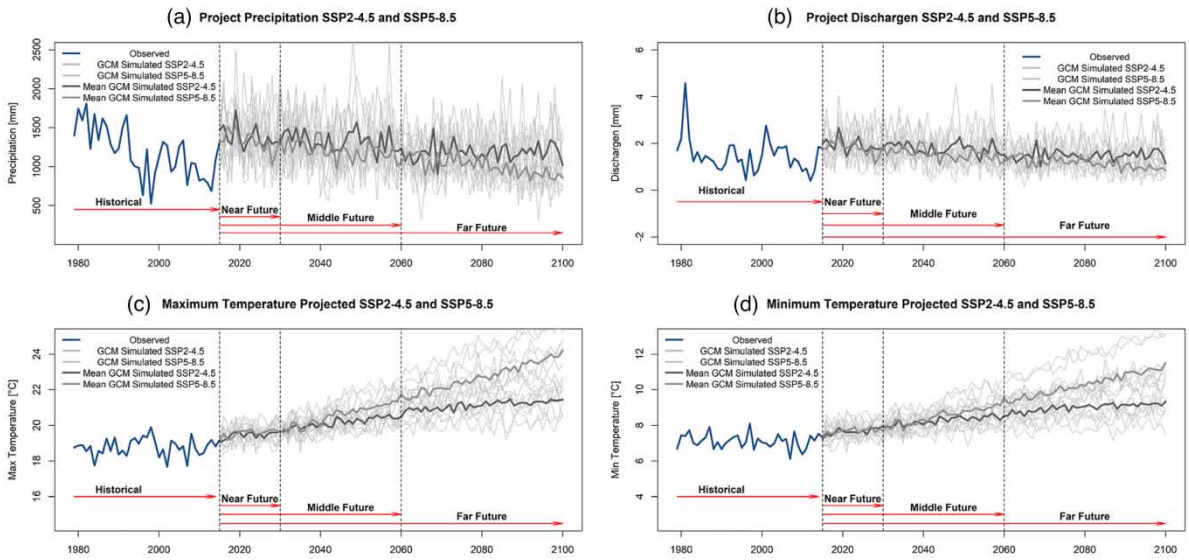

Figure 7 | SSP2-4.5 and SSP5-8.5 projections. (a) Precipitation; (b) discharge; (c) maximum temperature; and (d) minimum temperature.

5.2. Interannual variability

5.2.1. Seasonal variability

For the analysis of the expected seasonal variability, only the far future period (2015–2100) is considered since magnitudes of the hydrologic components are expected to steady in the long term. In this way, the climate change effects on hydrologic components can be evaluated for an extended period that will correspond to the most unfavorable condition for both SSP2-4.5 and SSP5-8.5.

The results of seasonal variability are shown in Table 4, where we can see that, for the austral summer, precipitation decreases by 27% in SSP2-4.5 and 54% in SSP5-8.5. In general, an increase in the maximum and minimum temperature is expected, regardless of the scenarios tested. In summer, the maximum temperature increase is expected to reach 6.5 °C at SSP5-8.5, while in winter less significant temperature variations may occur. Regarding discharge, in summer for SSP2-4.5, an increase of 33.7% is estimated, while in autumn for SSP5-8.5 an 83.7% decrease in discharge is expected.

5.2.2. Expected monthly variability

The results of the monthly variability of precipitation, maximum and minimum temperatures and flow showed that: Regarding precipitation, the most important decrease appears between June and August for SSP5-8.5, with increases during April and May for SSP2-4.5. The largest increases in maximum and minimum temperatures are estimated between March and July for both SSPs, while for November a decrease of 0.9 °C is projected for SSP2-4.5.

Figure 8 shows discharge (Figures 8(a) and 8(c)) and precipitation (Figures 8(b) and 8(d)) for the SSP2-4.5 and 8.5 scenarios. In the first scenario, there is less variability in both components, and they also follow similar seasonal trends in the projected periods. However, there is an advance in downloading, with the peak in July rather than August. This is mainly due to the rainfall regime of the basin, in which floods are produced by rains that have the same delay along with discharge. These changes in the timing of seasonal discharge suggest that there are likely to be significant effects on water resources, including water supply (municipal, industrial and irrigated).

The hydrologic components evaluated in SWAT+ are ET, PERC, SURQ, subsurface runoff (LATQ), GWQ, and WYLD.

Figures 9(a) and 9(c) show hydrologic components of the observed representative year (2015) in contrast to discharge (bar plot), while Figures 9(b) and 9(d) held for the worst representative year (2100). Here, we observe a directly proportional relationship between the hydrologic components and discharge, therefore, any variation on these components is also manifested in the discharge.

In the SSP5-8.5 scenario, there is a significant increase in discharge and also in hydrological components, which is due to the increase in extreme events in the basin. As for the SSP2-4.5 scenario, there is an extreme discharge offset that peaks in July instead of June.

5.3. Climate change projections considering extreme events

Modeling results using the SSP2-4.5 and SSP5-8.5 projections for the components of the hydrological cycle are presented in Table 5. Here, we consider discarded extreme events as being outside the 5th and 95th percentiles. We can see that in the entire period under the SSP2-8.5 scenario, there is an increase in discharge. This does not mean that this variable increases steadily over time, but that incorporating extreme events generates localized floods in the time ranges analyzed.

With SSP5-8.5, there is a similar response, except for the 2005–2100 period, which, even with extreme precipitation, generates a decrease in discharge. This leads to the conclusion that this period continues to be the most unfavorable one.

Table 4 | Seasonal variability for SSP2-4.5 and SSP5-8.5

Seasonal variability

	Precipitation		T_{max} (°C)		T_{min} (°C)		Discharge	
Seasons	**4.5**	**8.5**	**4.5**	**8.5**	**4.5**	**8.5**	**4.5**	**8.5**
Summer	−27.6%	−54.8%	3.3	6.5	1.6	3.7	33.7%	−17.4%
Autumn	20.5%	−9.8%	2.4	4.6	2.7	4.9	−8.6%	−83.7%
Winter	8.7%	−31.6%	2.3	4.3	2.5	4.4	7.4%	−63.6%
Spring	23.3%	−9.9%	2.8	5.6	2.0	3.7	30.9%	−43.8%

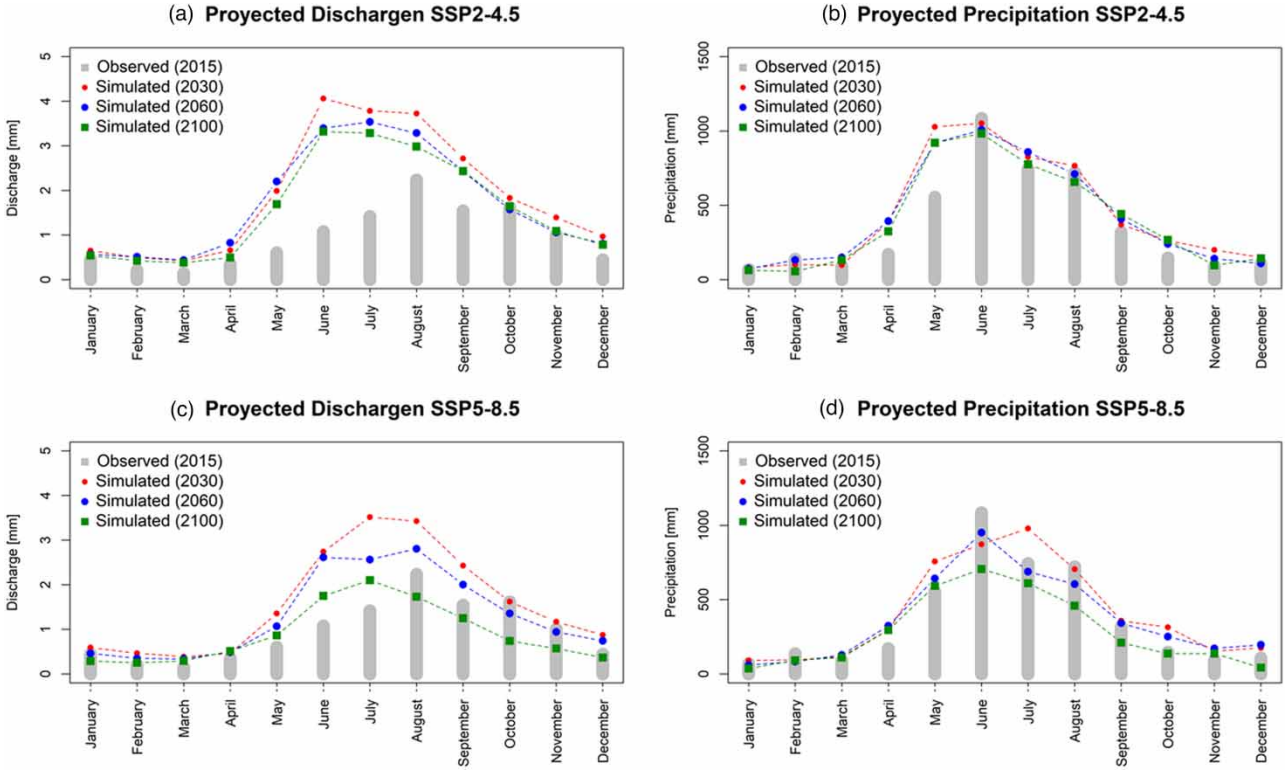

Figure 8 | (a) Monthly discharge projections in SSP2-4.5, (b) monthly precipitation projections in SSP2-4.5, (c) monthly discharge projections in SSP5-8.5, and (d) monthly precipitation projections in SSP5-8.5.

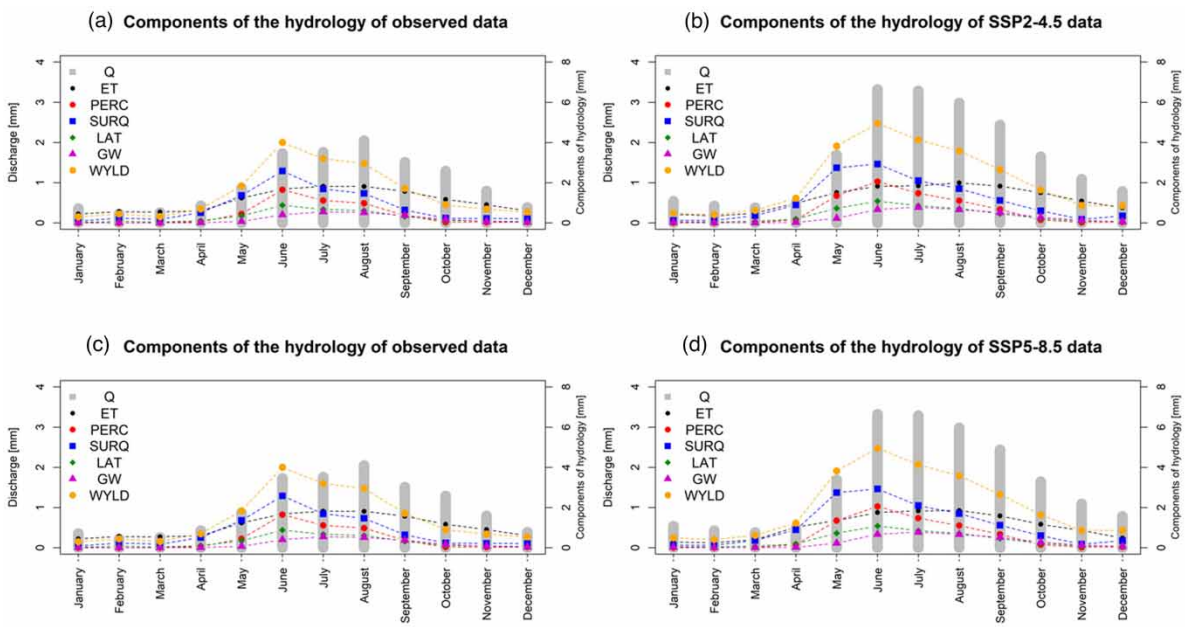

Figure 9 | (a) Monthly values of the hydrological components for observed data, (b) monthly values of the hydrologic components for SSP2-4.5, (c) monthly values of the hydrologic components for observed data, and (d) monthly values of the hydrologic components for SSP5-8.5.

Table 5 | Percentage variation of the different hydrological components

Hydrologic components	2005–2025		2005–2050		2005–2100	
	4.5	8.5	4.5	8.5	4.5	8.5
Q (Discharge)	49.49%	40.09%	45.36%	27.79%	40.68%	−5.45%
ET (Evapotranspiration)	16.30%	15.96%	15.27%	14.33%	13.90%	1.53%
PERC (Percolation)	55.75%	45.75%	49.59%	34.03%	46.17%	1.74%
SURQ (Surface runoff)	46.11%	39.48%	44.03%	30.99%	39.21%	5.59%
LATQ (Subsurface runoff)	46.15%	37.38%	41.78%	27.86%	37.54%	0.24%
GWQ (Groundwater)	55.65%	45.83%	49.58%	33.92%	46.33%	1.86%
WYLD	48.94%	40.80%	45.29%	31.23%	41.01%	3.95%

In addition, as seen above, the discharge has a direct relationship with the other hydrological components where we highlight PERC and GWQ that have similar variations, and SURQ which is generally greater than LATQ, due to the type of soil and the fact that the response time in a flood event is shorter, which does not allow water infiltration.

6. DISCUSSION

In this study, a comprehensive method for evaluating the effects of climate change on hydrological components using the SWAT+ model is presented. Evaluating the impact of climate change on hydrology and water resources has some limitations and uncertainties. Both the limitations and the uncertainties can be found at different stages of the methodological application: from the hydrological modeling, related to the different shares socioeconomic pathway (SSP) and the different GCMs, to the downscaling process and its projected results (Ouyang *et al.* 2015). These limitations are discussed in the following.

6.1. Hydrological modeling uncertainty

Although the calibration and validation of SWAT+ show accurate precision, there is still uncertainty associated to the model spatial distribution, the input data, and its parameters (Yu *et al.* 2020).

This is since the hydrological cycle has a high level of uncertainty in each of its processes (Dimitriadis *et al.* 2021) and this added to the fact that daily data are not available for some climatic variables, such as solar radiation, relative humidity and wind speed. These variables were obtained by a stochastic meteorological generator within the SWAT+ model based on the monthly statistics from the surrounding meteorological stations in the study area (Ouyang *et al.* 2015). Such gap-filling data could increase the modeling uncertainty. However, they help to overcome the lack of data problem, allowing hydrologic simulations when sufficient public meteorological data is available (Čerkasova *et al.* 2018).

SWAT+ calibration results are highly influenced by the model objective function, since it inherits the uncertainty associated with the above-mentioned gap-filling meteorological data. This means that the final simulated data have the same drawbacks, affecting the statistical indicators. For example, NSE and R^2 are more sensitive to high discharge than to low discharge (Legates & McCabe 1999). This makes a better model calibration performance in the wet period.

6.2. Uncertainty related to shared SSP and GCMs

There is a great uncertainty regarding how future greenhouse gases behave, as well as how the response of the global and regional climate system will be in these emission scenarios (Stehr *et al.* 2008).

According to the IPCC, the global temperature difference between the CMPI6 scenarios is the major source of uncertainty at the end of the 21st century (Scafetta 2024). This is associated with GCM capability to simulate future climates; even if it adequately simulates the current one, it may not be as reliable for future climate projections. To reduce this uncertainty, GCM ensembles are usually used (Cabré 2011) rather than the use of few GCMs that not provide a representative sample of the entire range of uncertainty. Therefore, GCM ensembles can help determine whether the projected changes are significant, considering the uncertainty of the model. The next generation of global climate models may improve current results (Araya-Osses *et al.* 2020) as they consider more variables. One of the variables to consider may be changes in land use,

therefore, it would be interesting to combine scenarios of land use changes with climate change projections that are available at the time of carrying out said investigation.

6.3. Downscaling method uncertainty

Advances in local prediction capacity and the evaluation of the potential climate change effects on water availability and distribution provide a real capacity to improve water resource management (Stehr *et al.* 2008). One of the primary sources of error in future climate projections is to assume that the daily precipitation time series that occurs or not in the future is identical to the past one, without modifying the occurrence and distribution of future precipitation. The weights based on the grid distance used for downscaling are also a major source of uncertainty (Ouyang *et al.* 2015).

6.4. Results

The results show a decrease in projected precipitation ranging between 9.8 and 54.8% for different periods. This agrees with previous studies like Christensen 2007 and Quintana & Aceituno 2012 that conclude that precipitation will have changes in its spatial and temporal distribution. Also, GCM simulations show precipitation decreases between 10 and 30% that are expected in south-central Chile at the end of the century (2080–2100) (Valdés-Pineda *et al.* 2014). According to Araya-Osses *et al.* (2020), decreases in winter precipitation over 40% are projected, while precipitation projections for two basins in the Bio-Bio region, Vergara and Lonquimay rivers, will decrease between the years 2071 and 2100 in 15.4 and 33.5%, respectively (Stehr *et al.* 2008).

Average air temperature variations between 2.4 and 4.7 °C are expected in the study area, for SSP2-4.5 and SSP5-8.5. This figure is higher than that obtained in a study carried out by Stehr *et al.* (2008) in two basins near the Andalién River in the Bío-Bío Region (Lonquimay River basin and Vergara River basin), in which temperature values ranged between 2 and 3.5 °C (Stehr 2008).

Discharge projection has the greater variation, increasing up to 33.7% in some periods and decreasing up to 83.7% in others. According to Carrasco *et al.* (2005, 2008), this is because of discharge fluctuations triggered by changes in glacier melting, depending on the season (Pizarro *et al.* 2013). In the same context, Pizarro *et al.* (2014) compared the maximum annual discharge in 30 years, observing an average increase of 22.6%. In simulated studies performed in the Bio-Bio Region, we can also see a wide range of variations for the future annual average discharge (from −81 to +7%) (Stehr *et al.* 2010). This is in line with what was studied by Blöschl *et al.* (2019), where it is mentioned that variability in discharge remains controversial, since there are individual extreme events that do not represent an increase in discharge in the long term, but rather it is decreasing (Blöschl *et al.* 2019). On the other hand, it should be noted that Pizarro mentions that although future projections show a great variation in discharge levels, this is not consistent with the data observed in the records; they have not shown patterns of change in a consistent way (Pizarro *et al.* 2022), and it is possible that the differences in the findings are related to the methodologies used and local effects. Additionally, we believe that the results of our study can be generalized to basins with characteristics similar to those of the Andalién River.

In this study, a high variation in the components of hydrology is shown, although this variation agrees with the other elements, such as precipitation, maximum and minimum temperature; in other studies, it is mentioned that the components of hydrology should not vary since the behavior of the Humboldt current, which could intensify with climate change, by cooling surface waters near the coast of Chile. The Humboldt current produces a cooling effect on the air masses that enter the continent from the ocean, neutralizing global warming in the coastal strip (Araya-Osses *et al.* 2020).

Notably, the greater variation observed in the SSP5-8.5 scenario in certain seasons and months can be attributed to a combination of factors. First, the SSP5-8.5 scenario represents a higher emissions trajectory, which tends to amplify the sensitivity of the regional climate system (Meinshausen *et al.* 2020). This increased sensitivity results in stronger responses to greenhouse gas forcing during specific periods, such as summer and winter, when temperature and precipitation patterns are more likely to show pronounced variability, which typically occurs in warm, Mediterranean-type climates such as the Andalien Basin. In addition, the parameters used in the model, particularly those related to temperature, are more reactive in higher emissions scenarios, leading to greater variations in the results.

7. CONCLUSION

An evaluation of climate change is performed successfully in the coastal basin of Central Chile. This was achieved by analyzing the effects of two climate change scenarios at medium (SSP2-4.5) and high (SSP5-8.5) emission of greenhouse gases, using

ensembles of ten CMIP6 models. Using a GCM ensemble is recommended to reduce the different sources of uncertainty and to analyze the robustness of the results (Araya-Osses *et al.* 2020). Subsequently, the simulated data are downscaled by using a Quantile Mapping Bias Correction method that provides precipitation and temperature projections. The latter allowed the development of the SWAT+ hydrological model applied to the Andalién river basin that estimates the effects in the hydrological cycle under the projected meteorological conditions, thus evaluating the effects associated with climate change (Garreaud 2011).

In this study, we found a constant temperature increase in both SSPs. A decrease in rainfall is also observed in some months, while in others an increase in rainfall is seen. This translates into flooding due to spillage during certain months, which is consistent with other studies, as seen above. The consequences of these variations might cause basin droughts (mainly in the dry season), and flooding problems previously seen in the Andalién river basin (Knutti *et al.* 2010). These conditions, added to the mega-drought that affects this area (Muñoz *et al.* 2020b), can affect human life in the towns along the Andalién river (Serur & Sarma 2018). Therefore, it is recommended to update flood studies with the new projected hydrological conditions in order to estimate the impacts of future extreme events. Additionally, this will help determine if the existing hydraulic structures (designed for different hydrological conditions) may be affected or overwhelmed by these extreme events. On the other hand, it is suggested to carry out studies of climate change projections in basins adjacent to the Andalien River basin, which include sediment transport and changes in land use.

After a few decades, depending on the characteristics of the basin and climate change scenarios, the total flow of this basin will fall below the current level, but the number of extreme events will increase in frequency and intensity. For this reason, decision makers must plan reasonable strategies based on watershed characteristics, for example land use changes, to adapt to the impact of climate change. (Luo *et al.* 2019) and thus reduce its consequences on ecosystems, agricultural production, and the risk of extinction of flora and fauna that therefore will reduce threats to food security and water resources (Araya-Osses *et al.* 2020). It is imperative to implement measures to take advantage of storing any excess water in the wet seasons to use it during dry seasons (Githui *et al.* 2009).

The predictions made could significantly contribute to decision-making regarding the future directions of water resource management policies and climate adaptation efforts. Integrating these predictions into local and regional government planning would enhance community resilience by enabling proactive measures and the sustainable management of water during drought periods. Although these results, like those of all studies on hydrology and climate change, present a certain degree of uncertainty, they highlight key trends that are undoubtedly useful for water resource planning.

DATA AVAILABILITY STATEMENT

Data cannot be made publicly available; readers should contact the corresponding author for details.

CONFLICT OF INTEREST

The authors declare there is no conflict.

REFERENCES

Araya-Osses, D., Casanueva, A., Román-Figueroa, C., Uribe, J. M. & Paneque, M. (2020) Climate change projections of temperature and precipitation in Chile based on statistical downscaling, *Climate Dynamics*, **54** (9–10), 4309–4330. https://doi.org/10.1007/s00382-020-05231-4.

Arnold, J. G., Srinivasan, R., Muttiah, R. S. & Williams, J. R. (1998) *LARGE AREA HYDROLOGIC MODELING AND ASSESSMENT PART I : MODEL DEVELOPMENT ' basin scale model called SWAT (Soil and Water speed and storage, advanced software debugging policy to meet the needs, and the management to the tank model (Sugawara et al., 1. 34*(1), 73–89.

Ayivi, F. & Jha, M. K. (2018) Estimation of water balance and water yield in the Reedy Fork-Buffalo Creek Watershed in North Carolina using SWAT, *International Soil and Water Conservation Research*, **6** (3), 203–213. https://doi.org/10.1016/j.iswcr.2018.03.007.

Bae, D. H., Jung, I. W. & Lettenmaier, D. P. (2011) Hydrologic uncertainties in climate change from IPCC AR4 GCM simulations of the Chungju Basin, Korea, *Journal of Hydrology*, **401** (1–2), 90–105. https://doi.org/10.1016/j.jhydrol.2011.02.012.

Barrientos, G., Herrero, A., Iroumé, A., Mardones, O. & Batalla, R. J. (2020) Modelling the effects of changes in forest cover and climate on hydrology of headwater catchments in South-Central Chile, *Water*, **12** (6), 1828. https://doi.org/10.3390/w12061828.

Bauer, C. J. (2015) Water conflicts and entrenched governance problems in Chile's market model, *Water Alternatives*, **8** (2), 147–172.

Bieger, K., Arnold, J. G., Rathjens, H., White, M. J., Bosch, D. D., Allen, P. M., Volk, M. & Srinivasan, R. (2017) Introduction to SWAT+, A completely restructured version of the soil and water assessment tool, *JAWRA Journal of the American Water Resources Association*, **53** (1), 115–130. https://doi.org/10.1111/1752-1688.12482.

Blöschl, G., Hall, J., Viglione, A., Perdigão, R. A. P., Parajka, J., Merz, B., Lun, D., Arheimer, B., Aronica, G. T., Bilibashi, A., Boháč, M., Bonacci, O., Borga, M., Čanjevac, I., Castellarin, A., Chirico, G. B., Claps, P., Frolova, N., Ganora, D., Gorbachova, L., Gül, A., Hannaford, J., Harrigan, S., Kireeva, M., Kiss, A., Kjeldsen, T. R., Knijff, J., Kokkonen, T., Litvinov, V., Macdonald, N., Mavrova-Guirguinova, M., Mediero, L., Merz, R., Molnar, P., Montanari, A., Murphy, C., Osuch, M., Radevski, I., Salinas, J. L., Sauquet, E., Šraj, M., Szolgay, J., Volpi, E., Wilson, D., Zaimi, K. & Živković, N. (2019) Changing climate both increases and decreases European river floods, *Nature*, **573** (7772), 108–111. https://doi.org/10.1038/s41586-019-1495-6.

Brouziyne, Y., Abouabdillah, A., Bouabid, R., Benaabidate, L. & Oueslati, O. (2017) SWAT manual calibration and parameters sensitivity analysis in a semi-arid watershed in North-western Morocco, *Arabian Journal of Geosciences*, **10** (19), 427. https://doi.org/10.1007/s12517-017-3220-9.

Cabré, M. F. (2011) *Uso de un modelo climático regional para estimar el clima en Sudamérica subtropical para el futuro lejano. Estimación de incertidumbres del modelo*.

Calvin, K., Dasgupta, D., Krinner, G., Mukherji, A., Thorne, P. W., Trisos, C., Romero, J., Aldunce, P., Barrett, K., Blanco, G., Cheung, W. W. L., Connors, S., Denton, F., Diongue-Niang, A., Dodman, D., Garschagen, M., Geden, O., Hayward, B., Jones, C., Kang, Y., Laukkonen, J., Leitner, M., Mander, S., Mearns, E., Mechler, R., Morchain, D., Mustonen, T., Omukuti, J., Park, S. E., Rawlins, M. A., Rosenzweig, C., Santos, F. D., Schipper, L. F., Thomas, A., van Aalst, M., Vijayavenkataraman, S., Wignaraja, K., Wilbanks, T., Zommers, Z. & Ha, M. (2023) *IPCC, 2023: Climate Change 2023: Synthesis Report. Contribution of Working Groups I, II and III to the Sixth Assessment Report of the Intergovernmental Panel on Climate Change [Core Writing Team, H. Lee and J. Romero (eds.)]. IPCC, Geneva, Switzerland.* (P. Arias, M. Bustamante, I. Elgizouli, G. Flato, M. Howden, C. Méndez-Vallejo, J. J. Pereira, R. Pichs-Madruga, S. K. Rose, Y. Saheb, R. Sánchez Rodríguez, D. Ürge-Vorsatz, C. Xiao, N. Yassaa, J. Romero, J. Kim, E. F. Haites, Y. Jung, R. Stavins, & C. Péan, Eds.). https://doi.org/10.59327/IPCC/AR6-9789291691647.

Carrasco, J. F., Casassa, G. & Quintana, J. (2005) Changes of the 0°C isotherm and the equilibrium line altitude in central Chile during the last quarter of the 20th century, *Hydrological Sciences Journal*, **50** (6), 1–16. https://doi.org/10.1623/hysj.2005.50.6.933.

Carrasco, J. F., Osorio, R. & Casassa, G. (2008) Secular trend of the equilibrium-line altitude on the western side of the southern Andes, derived from radiosonde and surface observations, *Journal of Glaciology*, **54** (186), 538–550. https://doi.org/10.3189/002214308785837002.

Castillo, E. J. (2017) Geomorfología de la cuenca del río Andalién, Chile, *Revista Geográfica Del Instituto Panamericano de Geografía e Historia*, **143**, 97–116. https://doi.org/10.2307/40996764.

Čerkasova, N., Umgiesser, G. & Ertürk, A. (2018) Development of a hydrology and water quality model for a large transboundary river watershed to investigate the impacts of climate change – A SWAT application, *Ecological Engineering*, **124** (August), 99–115. https://doi.org/10.1016/j.ecoleng.2018.09.025.

Chen, Y., Marek, G. W., Marek, T. H., Moorhead, J. E., Heflin, K. R., Brauer, D. K., Gowda, P. H. & Srinivasan, R. (2019) Simulating the impacts of climate change on hydrology and crop production in the Northern High Plains of Texas using an improved SWAT model, *Agricultural Water Management*, **221** (November 2018), 13–24. https://doi.org/10.1016/j.agwat.2019.04.021.

Christensen, J. H. (2007) Regional climate projections. Chapter 11. In: S. Solomon, D. Qin, M. Manning, Z. Chen, M. Marquis, K. B. Averyt, M. Tignor, & H. L. Miller (Eds.) *Climate Change 2007: The Physical Science Basis. Contribution of Working Group I to the Fourth Assessment Report of the Intergovernmental Panel on Climate Change*. Cambridge, UK: Cambridge University Press, pp. 847–940. Available at: https://scholar.google.com/scholar_lookup?title=Climate change 2007%3A the physical science basis. Contribution of working group I to the fourth assessment report of the intergovernmental panel on climate change&publication_year=2007&author=Christensen%2C.

CONAF (2015) *Catastro y Evaluación de los Recursos Vegetacionales de Chile – Actualización*. Available at: https://ide.minagri.gob.cl/geoweb/2019/11/22/planificacion-catastral/

(DGA), D. Ge. de A. (2004). *Cuenca del rio andalien*.

Dimitriadis, P., Koutsoyiannis, D., Iliopoulou, T. & Papanicolaou, P. (2021) A global-scale investigation of stochastic similarities in marginal distribution and dependence structure of key hydrological-cycle processes, *Hydrology*, **8** (2), 59. https://doi.org/10.3390/hydrology8020059.

Eckhardt, K., Fohrer, N. & Frede, H. G. (2005) Automatic model calibration, *Hydrological Processes*, **19** (3), 651–658. https://doi.org/10.1002/hyp.5613.

Ehsan, M. A., Kucharski, F., Almazroui, M., Ismail, M. & Tippett, M. K. (2019) Potential predictability of Arabian peninsula summer surface air temperature in the North American multimodel ensemble, *Climate Dynamics*, **53** (7–8), 4249–4266. https://doi.org/10.1007/s00382-019-04784-3.

Escanilla-Minchel, R., Alcayaga, H., Soto-Alvarez, M., Kinnard, C. & Urrutia, R. (2020) Evaluation of the impact of climate change on runoff generation in an andean glacier watershed, *Water (Switzerland)*, **12** (12), 3547. https://doi.org/10.3390/w12123547.

Essa, Y. H., Hirschi, M., Thiery, W., El-Kenawy, A. M. & Yang, C. (2023) Drought characteristics in Mediterranean under future climate change, *Npj Climate and Atmospheric Science*, **6** (1), 133. https://doi.org/10.1038/s41612-023-00458-4.

Fowler, H. J., Blenkinsop, S. & Tebaldi, C. (2007) Linking climate change modelling to impacts studies: Recent advances in downscaling techniques for hydrological modelling, *International Journal of Climatology*, **27** (12), 1547–1578. https://doi.org/10.1002/joc.1556.

Garreaud, R. (2011) Cambio Climático: Bases Físicas e Impactos en Chile, *Revista Tierra Adentro-INIA*, **93**, 14.

Garreaud, R. D., Boisier, J. P., Rondanelli, R., Montecinos, A., Sepúlveda, H. H. & Veloso-Aguila, D. (2020) The central Chile mega drought (2010–2018): A climate dynamics perspective, *International Journal of Climatology*, **40** (1), 421–439. https://doi.org/10.1002/joc.6219.

Ghosh, S. & Mujumdar, P. P. (2008) Statistical downscaling of GCM simulations to streamflow using relevance vector machine, *Advances in Water Resources*, **31** (1), 132–146. https://doi.org/10.1016/j.advwatres.2007.07.005.

Githui, F., Gitau, W., Mutua, F. & Bauwens, W. (2009) Climate change impact on SWAT simulated streamflow in western Kenya, *International Journal of Climatology*, **29** (12), 1823–1834. https://doi.org/10.1002/joc.1828.

Glynis, K.-G., Iliopoulou, T., Dimitriadis, P. & Koutsoyiannis, D. (2021) Stochastic investigation of daily air temperature extremes from a global ground station network, *Stochastic Environmental Research and Risk Assessment*, **35** (8), 1585–1603. https://doi.org/10.1007/s00477-021-02002-3.

Gouveia, C. D., Rodrigues Torres, R., Marengo, J. A. & Avila-Diaz, A. (2022) Uncertainties in projections of climate extremes indices in South America via Bayesian inference, *International Journal of Climatology*, **42** (14), 7362–7382. https://doi.org/10.1002/joc.7650.

Ha, D. T. T., Ghafouri-Azar, M. & Bae, D.-H. (2019) Long-term variation of runoff coefficient during dry and wet seasons due to climate change, *Water*, **11** (11), 2411. https://doi.org/10.3390/w11112411.

Horton, R. E. (1933) The Rôle of infiltration in the hydrologic cycle, *Transactions, American Geophysical Union*, **14** (1), 446. https://doi.org/10.1029/TR014i001p00446.

Intergovernmental Panel on Climate Change (IPCC) (2023) *Climate Change 2022 – Impacts, Adaptation and Vulnerability*. Cambridge, UK: Cambridge University Press.

IPCC (2014) Cambio climático 2014: Informe de Síntesis. In: R. K. Pachauri & L. A. Meyer (Eds.) *Contribución de los Grupos de trabajo I,II y III al Quinto Informe de Evaluación del Grupo Intergubernamental de Expertos sobre el Cambio Climático*. Geneva, Switzerland: Intergovernmental Panel on Climate Change.

Is-Enes (2021). *Infrastructure for the European Network for Earth System Modelling*. Available at: https://climate4impact.eu/impactportal/data/esgfsearch.jsp#.

Kassaye, S. M., Tadesse, T., Tegegne, G. & Hordofa, A. T. (2024) Quantifying the climate change impacts on the magnitude and timing of hydrological extremes in the Baro River Basin, Ethiopia, *Environmental Systems Research*, **13** (1), 2. https://doi.org/10.1186/s40068-023-00328-1.

Knutti, R., Furrer, R., Tebaldi, C., Cermak, J. & Meehl, G. A. (2010) Challenges in combining projections from multiple climate models, *Journal of Climate*, **23** (10), 2739–2758. https://doi.org/10.1175/2009JCLI3361.1.

Kottek, M., Grieser, J., Beck, C., Rudolf, B. & Rubel, F. (2006) World Map of the Köppen-Geiger climate classification updated, *Meteorologische Zeitschrift*, **15** (3), 259–263. https://doi.org/10.1127/0941-2948/2006/0130.

Kouchi, D. H., Esmaili, K., Faridhosseini, A., Sanaeinejad, S. H., Khalili, D. & Abbaspour, K. C. (2017) Sensitivity of calibrated parameters and water resource estimates on different objective functions and optimization algorithms, *Water*, **9** (6), 384. https://doi.org/10.3390/w9060384.

Koutsoyiannis, D. (2020) Revisiting the global hydrological cycle: Is it intensifying?, *Hydrology and Earth System Sciences*, **24** (8), 3899–3932. https://doi.org/10.5194/hess-24-3899-2020.

Lee, A., Cho, S., Kang, D. K. & Kim, S. (2014) Analysis of the effect of climate change on the Nakdong river stream flow using indicators of hydrological alteration, *Journal of Hydro-Environment Research*, **8** (3), 234–247. https://doi.org/10.1016/j.jher.2013.09.003.

Legates, D. R. & McCabe, G. J. (1999) Evaluating the use of 'goodness-of-fit' measures in hydrologic and hydroclimatic model validation, *Water Resources Research*, **35** (1), 233–241. https://doi.org/10.1029/1998WR900018.

Lu, E., Takle, E. S. & Manoj, J. (2010) The relationships between climatic and hydrological changes in the Upper Mississippi River Basin: A SWAT and multi-GCM study, *Journal of Hydrometeorology*, **11** (2), 437–451. https://doi.org/10.1175/2009JHM1150.1.

Luo, M., Liu, T., Meng, F., Duan, Y., Bao, A., Xing, W., Feng, X., De Maeyer, P. & Frankl, A. (2019) Identifying climate change impacts on water resources in Xinjiang, China, *Science of the Total Environment*, **676**, 613–626. https://doi.org/10.1016/j.scitotenv.2019.04.297.

Meinshausen, M., Nicholls, Z. R. J., Lewis, J., Gidden, M. J., Vogel, E., Freund, M., Beyerle, U., Gessner, C., Nauels, A., Bauer, N., Canadell, J. G., Daniel, J. S., John, A., Krummel, P. B., Luderer, G., Meinshausen, N., Montzka, S. A., Rayner, P. J., Reimann, S., Riahi, K., Rogelj, J., Séférian, R., Smith, S. J., Steinberger, J., van Vuuren, D. P., Voulgarakis, A. & Wang, R. H. J. (2020) The shared socio-economic pathway (SSP) greenhouse gas concentrations and their extensions to 2500, *Geoscientific Model Development*, **13** (8), 3571–3605. https://doi.org/10.5194/gmd-13-3571-2020.

Mengistu, A. G., van Rensburg, L. D. & Woyessa, Y. E. (2019) Techniques for calibration and validation of SWAT model in data scarce arid and semi-arid catchments in South Africa, *Journal of Hydrology: Regional Studies*, **25**, 100621. https://doi.org/10.1016/j.ejrh.2019.100621.

Morbidelli, R., Corradini, C., Saltalippi, C., Flammini, A., Dari, J. & Govindaraju, R. (2018) Rainfall infiltration modeling: A review, *Water*, **10** (12), 1873. https://doi.org/10.3390/w10121873.

Muñoz, A. A., Klock-Barría, K., Alvarez-Garreton, C., Aguilera-Betti, I., González-Reyes, Á., Lastra, J. A., Chávez, R. O., Barría, P., Christie, D., Rojas-Badilla, M. & Lequesne, C. (2020a) Water crisis in petorca basin, Chile: The combined effects of a mega-drought and water management, *Water (Switzerland)*, **12** (3), 648. https://doi.org/10.3390/w12030648.

Muñoz, A. A., Klock-Barría, K., Alvarez-Garreton, C., Aguilera-Betti, I., González-Reyes, Á., Lastra, J. A., Chávez, R. O., Barría, P., Christie, D., Rojas-Badilla, M. & Lequesne, C. (2020b) Water crisis in petorca basin, Chile: The combined effects of a mega-drought and water management, *Water (Switzerland)*, **12** (3), 1–18. https://doi.org/10.3390/w12030648.

Orellana, C. P., Escanilla-Minchel, R., Cortes, A. G., Alcayaga, H., Aguayo, M., Aguayo, M. A. & Flores, A. N. (2022) Assessment of future land use/land cover scenarios on the hydrology of a coastal basin in South-Central Chile, *Sustainability*, **14** (24), 16363. https://doi.org/10.3390/su142416363.

Oti, J. O., Kabo-bah, A. T. & Ofosu, E. (2020) Hydrologic response to climate change in the Densu River Basin in Ghana, *Heliyon*, **6** (8), e04722. https://doi.org/10.1016/j.heliyon.2020.e04722.

Ouyang, F., Zhu, Y., Fu, G., Lü, H., Zhang, A., Yu, Z. & Chen, X. (2015) Impacts of climate change under CMIP5 RCP scenarios on streamflow in the Huangnizhuang catchment, *Stochastic Environmental Research and Risk Assessment*, **29** (7), 1781–1795. https://doi.org/10.1007/s00477-014-1018-9.

Pérez-Sánchez, J., Senent-Aparicio, J., Santa-María, C. M. & López-Ballesteros, A. (2020) Assessment of ecological and hydro-geomorphological alterations under climate change using SWAT and IAHRIS in the Eo River in Northern Spain, *Water (Switzerland)*, **12** (6), 1–31. https://doi.org/10.3390/W12061745.

Pierce, D. W., Barnett, T. P., Santer, B. D. & Gleckler, P. J. (2009) Selecting global climate models for regional climate change studies, *Proceedings of the National Academy of Sciences of the United States of America*, **106** (21), 8441–8446. https://doi.org/10.1073/pnas.0900094106.

Pizarro, A., Dimitriadis, P., Iliopoulou, T., Manfreda, S. & Koutsoyiannis, D. (2022) Stochastic analysis of the marginal and dependence structure of streamflows: From fine-scale records to multi-centennial paleoclimatic reconstructions, *Hydrology*, **9** (7), 126. https://doi.org/10.3390/hydrology9070126.

Pizarro, R., Garcia-Chevesich, P., Valdes, R., Dominguez, F., Hossain, F., Ffolliott, P., Olivares, C., Morales, C., Balocchi, F. & Bro, P. (2013) Inland water bodies in Chile can locally increase rainfall intensity, *Journal of Hydrology*, **481**, 56–63. https://doi.org/10.1016/j.jhydrol.2012.12.012.

Pizarro, R., Vera, M., Valdés, R., Helwig, B. & Olivares, C. (2014) Multi-decadal variations in annual maximum peak flows in semi-arid and temperate regions of Chile, *Hydrological Sciences Journal*, **59** (2), 300–311. https://doi.org/10.1080/02626667.2013.803182.

Quintana, J. M. & Aceituno, P. (2012) Changes in the rainfall regime along the extratropical west coast of South America (Chile): 30-43o S, *Atmósfera*, 25 (1), 1–22.

Scafetta, N. (2024) Impacts and risks of 'realistic' global warming projections for the 21st century, *Geoscience Frontiers*, **15** (2), 101774. https://doi.org/10.1016/j.gsf.2023.101774.

Serur, A. B. & Sarma, A. K. (2018) Climate change impacts analysis on hydrological processes in the Weyib River basin in Ethiopia, *Theoretical and Applied Climatology*, **134** (3–4), 1301–1314. https://doi.org/10.1007/s00704-017-2348-6.

Stehr, A. (2008) *Análisis del comportamiento hidrológico y disponibilidad de agua, bajo escenarios de cambio climático, para dos sub-cuencas del río Biobío incorporando el impacto del aporte nival en la zona cordillerana*, p. 123.

Stehr, A., Debels, P., Romero, F. & Alcayaga, H. (2008) Hydrological modelling with SWAT under conditions of limited data availability: Evaluation of results from a Chilean case study, *Hydrological Sciences Journal*, **53** (3), 588–601. https://doi.org/10.1623/hysj.53.3.588.

Stehr, A., Debels, P., Arumi, J. L., Alcayaga, H. & Romero, F. (2010) Modelling hydrological response to climate change: Experiences from two South – Central Chilean watersheds, *Tecnologia y Ciencias Del Agua*, **1** (4), 37–58.

Stolpe, N. (2006) *Descripción de los principales suelos de la VIII Región de Chile. May 2006*.

Tan, M. L., Ibrahim, A. L., Yusop, Z., Chua, V. P. & Chan, N. W. (2017) Climate change impacts under CMIP5 RCP scenarios on water resources of the Kelantan River Basin, Malaysia, *Atmospheric Research*, **189**, 1–10. https://doi.org/10.1016/j.atmosres.2017.01.008.

Tebaldi, C. & Knutti, R. (2007) The use of the multi-model ensemble in probabilistic climate projections, *Philosophical Transactions of the Royal Society A: Mathematical, Physical and Engineering Sciences*, **365** (1857), 2053–2075. https://doi.org/10.1098/rsta.2007.2076.

Torres, R., Azócar, G., Rojas, J., Montecinos, A. & Paredes, P. (2015) Vulnerability and resistance to neoliberal environmental changes: An assessment of agriculture and forestry in the Biobio region of Chile (1974–2014), *Geoforum*, **60**, 107–122. https://doi.org/10.1016/j.geoforum.2014.12.013.

Tramblay, Y., Koutroulis, A., Samaniego, L., Vicente-Serrano, S. M., Volaire, F., Boone, A., Le Page, M., Llasat, M. C., Albergel, C., Burak, S., Cailleret, M., Kalin, K. C., Davi, H., Dupuy, J.-L., Greve, P., Grillakis, M., Hanich, L., Jarlan, L., Martin-StPaul, N., Polcher, J., Ribes, A., Seiradakis, K., Tourre, Y. M., Vannière, B. & Vidal, J.-P. (2020) Challenges for drought assessment in the Mediterranean region under future climate scenarios, *Earth-Science Reviews*, **210**, 103348. https://doi.org/10.1016/j.earscirev.2020.103348.

Valdés-Pineda, R., Pizarro, R., García-Chevesich, P., Valdés, J. B., Olivares, C., Vera, M., Balocchi, F., Pérez, F., Vallejos, C., Fuentes, R., Abarza, A. & Helwig, B. (2014) Water governance in Chile: Availability, management and climate change, *Journal of Hydrology*, **519**, 2538–2567. https://doi.org/10.1016/j.jhydrol.2014.04.016.

Verichev, K., Zamorano, M. & Carpio, M. (2020) Effects of climate change on variations in climatic zones and heating energy consumption of residential buildings in the southern Chile, *Energy and Buildings*, **215**, 109874. https://doi.org/10.1016/j.enbuild.2020.109874.

von Storch, H., Zorita, E. & Cubasch, U. (1993) Downscaling of global climate change estimates to regional scales: An application to Iberian rainfall in wintertime, *Journal of Climate*, **6** (6), 1161–1171. https://doi.org/10.1175/1520-0442(1993)006<1161:DOGCCE>2.0.CO;2.

Vozinaki, A.-E. K., Tapoglou, E. & Tsanis, I. K. (2018) Hydrometeorological impact of climate change in two Mediterranean basins, *International Journal of River Basin Management*, **16** (2), 245–257. https://doi.org/10.1080/15715124.2018.1437742.

Wangpimool, W., Pongput, K., Sukvibool, C., Sombatpanit, S. & Gassman, P. W. (2013) The effect of reforestation on stream flow in Upper Nan river basin using Soil and Water Assessment Tool (SWAT) model, *International Soil and Water Conservation Research*, **1** (2), 53–63. https://doi.org/10.1016/S2095-6339(15)30039-3.

Welde, K. & Gebremariam, B. (2017) Effect of land use land cover dynamics on hydrological response of watershed: Case study of Tekeze Dam watershed, northern Ethiopia, *International Soil and Water Conservation Research*, **5** (1), 1–16. https://doi.org/10.1016/j.iswcr.2017.03.002.

Wu, J., Yen, H., Arnold, J. G., Yang, Y. C. E., Cai, X., White, M. J., Santhi, C., Miao, C. & Srinivasan, R. (2020) Development of reservoir operation functions in SWAT+ for national environmental assessments, *Journal of Hydrology*, **583**, 124556. https://doi.org/10.1016/j.jhydrol.2020.124556.

Yu, Z., Man, X., Duan, L. & Cai, T. (2020) Assessments of impacts of climate and forest change onwater resources using swatmodel in a subboreal watershed in northern da hinggan mountains, *Water (Switzerland)*, **12** (6), 1565. https://doi.org/10.3390/W12061565.

First received 16 May 2024; accepted in revised form 25 November 2024. Available online 2 December 2024